Journal of Engineering Mathematics 21: 115–127 (1987)

On the structural stability of a simple pooled chemical system

J.H. MERKIN, [1] D.J. NEEDHAM [2] and S.K. SCOTT [3]
[1] *Department of Applied Mathematics, University of Leeds, Leeds LS2 9JT, England;*
[2] *School of Mathematics and Physics, University of East Anglia, Norwich NR4 7TJ, England;*
[3] *Department of Physical Chemistry, University of Leeds, Leeds LS2 9JT, England*

Received 13 November 1986; accepted 22 December 1986

Abstract

The effect of adding the uncatalysed reaction step to the cubic autocatalator in a closed system is examined under the pooled chemical approximation. The addition of this extra step has a dramatic effect on the overall reaction over the parameter range where, without this step, the pooled chemical approximation breaks down. It is found that, no matter how slow the uncatalysed reaction, the pooled chemical approximation now remains valid throughout. There is a parameter range where there is oscillatory behaviour, these oscillations arising from points of Hopf bifurcation.

1. Introduction

In this paper we consider the prototype chemical reaction scheme based on the cubic autocatalator, with the reactant A produced by a simple first order decay from a precursor P. The reaction scheme is

$$\mathrm{P} \rightarrow \mathrm{A} \qquad \text{rate } k_0 p \tag{1}$$

$$\mathrm{A} + 2\mathrm{B} \rightarrow 3\mathrm{B} \qquad \text{rate } k_1 ab^2 \tag{2}$$

$$\mathrm{B} \rightarrow \mathrm{C} \qquad \text{rate } k_2 b \tag{3}$$

(where p, a and b are the concentrations of P, A and B respectively and k_0, k_1 and k_2 are the rate constants). It has been shown, Gray and Scott [1,2,3], Scott [4] and D'Anna et al. [5], that the reaction scheme given by (2) and (3) can, in an open system (the continuous stirred tank reactor (c.s.t.r.)), display many complex patterns of behaviour. Here we suppose that the reaction is taking place within a closed system, with the continuous supply of fresh reactant A in the c.s.t.r. being replaced by the production of A from P via step (1). Consequent on this is the assumption that the initial concentration of P is many orders of magnitude greater than the concentrations of the intermediates A and B. This problem has been discussed by the authors, Merkin et al. [6], allowing for the very slow reduction in the concentration of P.

However, in such a situation (where one of the reactants is initially present in large excess) it is common to invoke the "pooled chemical approximation" which, in the present context, means assuming that the concentration of P remains constant throughout. The consequences of doing this for reaction scheme (1–3) have been discussed in Merkin et al. [7], where it was shown that taking the concentration of P as a constant is a good approximation initially, with p taking its local slowly decaying value. However, as time elapses this quasi-steady state becomes unstable, oscillations then develop which grow in amplitude and period until after a further

time the concentration of A grows unbounded (and that of B decreases to zero). The pooled chemical approximation has then broken down.

Merkin et al. [6] showed that the addition of the slow uncatalysed step

$$A \to B \quad \text{rate } k_3 a \tag{4}$$

had a dramatic effect on the overall reaction. This extra step enables B to be formed (even though this rate of production may be very slow) and this acts as a trigger for the much faster autocatalytic step (2). The effect of allowing an uncatalysed reaction to take place in parallel with the autocatalytic process has been investigated in considerable detail in the c.s.t.r. context, B.F. Gray et al. [8], B.F. Gray and Scott [9].

The purpose of this paper is to consider the reaction scheme (1)–(4) under the pooled chemical approximation, i.e. assuming that the concentration of P remains constant. We show that, with the inclusion of the uncatalysed step (4), the concentrations of A and B remain bounded throughout. Thus this slight modification to the original reaction scheme enables the pooled chemical approximation to remain valid over the whole parameter range. There is still a parameter range over which oscillations occur, with these oscillations arising from limit cycles created at two points of Hopf bifurcation. We see that at both these points the bifurcation produces a stable limit cycle, enabling us to conclude that there is just one stable limit cycle possible, existing over the parameter range for which the stationary state is unstable.

2. Equations

From Merkin et al. [6], the equations describing the reaction scheme (1–4), assuming the the concentration of P remains constant at its initial value p_0, are

$$\frac{dx}{dt} = \mu - xy^2 - \frac{x}{\rho}, \quad \frac{dy}{dt} = xy^2 - y + \frac{x}{\rho} \tag{5}$$

in $x \geqslant 0$, $y \geqslant 0$. Here $x = (k_1/k_2)^{1/2}a$, $y = (k_1/k_2)^{1/2}b$ are the non-dimensional concentrations of A and B respectively, $t = k_2\bar{t}$ (where $\bar{t}$ is time), $\mu = (k_1/k_2)^{1/2}k_0p_0/k_2$ and $\rho = k_2/k_3$. The pooled chemical approximation means that μ is to be taken as a constant, of O(1), and the inclusion of the slow uncatalysed step (4) implies that the constant ρ is to be assumed large.

Equations effectively the same as (5) have been used by Tyson and Kauffman [10] and Ashkenazi and Othmer [11] in the context of cell division or mitosis, in which the reaction is assumed to take place in two compartments coupled by diffusion through a semi-permeable membrane. From Ashkenazi and Othmer [11] we have, in the notation of the present paper, that equations (5) have just one finite equilibrium point (x_s, y_s) where

$$x_s = \frac{\mu}{\mu^2 + \dfrac{1}{\rho}}, \quad y_s = \mu. \tag{6}$$

The locus of (x_s, y_s) as μ is varied is thus $x_s = y_s/(y_s^2 + 1/\rho)$ which is shown in Fig. 1, where we see that the effect of including the uncatalysed step is for both x_s and $y_s \to 0$ as $\mu \to 0$ (whereas without step (4) $x_s \to \infty$ as $\mu \to 0$).

For $\rho > 8$ there are Hopf bifurcations at (x_s, y_s) when $\mu = \mu_1$ and $\mu = \mu_2$, with $0 < \mu_1 < \mu_2 < 1$ and where

$$\mu_1^2 = \frac{1}{2}\left(1 - \frac{2}{\rho} - \sqrt{1 - \frac{8}{\rho}}\right), \quad \mu_2^2 = \frac{1}{2}\left(1 - \frac{2}{\rho} + \sqrt{1 - \frac{8}{\rho}}\right), \tag{7}$$

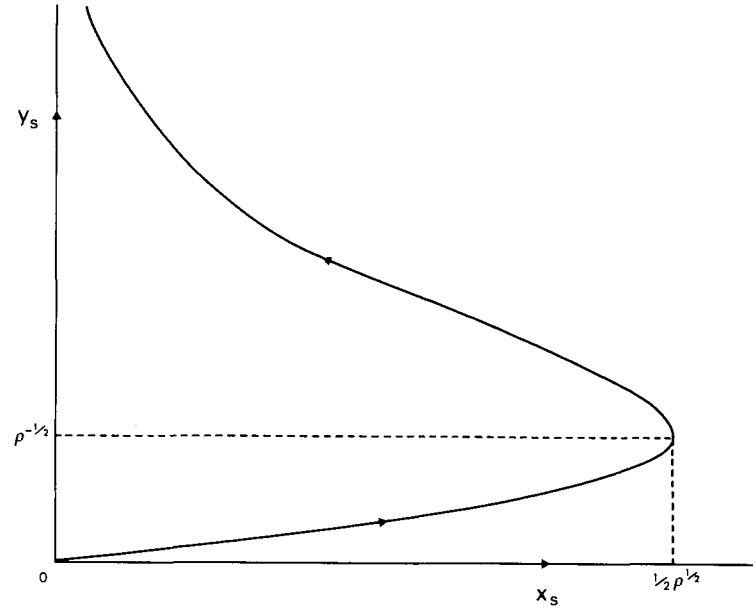

Fig. 1. A graph of the stationary state (x_s, y_s) as given parametrically by (6), the arrow indicates the direction of μ increasing.

so that for $\rho \gg 1$

$$\mu_1 \sim \rho^{-1/2} + \cdots, \quad \mu_2 \sim 1 - \frac{3}{2\rho} + \cdots. \tag{8}$$

The degenerate Hopf bifurcation at $\rho = 8$ has been studied by Golubitsky and Langford [12] in the context of singularity theory. The unfolding of the singularity at $\rho = 8$ showed that, close to $\rho = 8$ at least, there was just one limit cycle which existed in $\mu_1 < \mu < \mu_2$ and was stable. In the application we have in mind $\rho \gg 1$, and we can show that this situation of just one stable limit cycle existing for $\mu_1 < \mu < \mu_2$ persists for all $\rho > 8$, no matter how large the value of ρ (provided only that if remains finite). This is, perhaps, a little unexpected as in the c.s.t.r. context the type of bifurcation can change as the typical time for the decay of B varies, [3], with both stable and unstable limit cycles being possible.

Finally, we note that without the uncatalysed step, i.e. with ρ formally allowed to be infinite, there is just one point of Hopf bifurcation, at $\mu = 1$, producing a stable limit cycle in $\mu < 1$, which is destroyed at infinite amplitude by a heteroclinic orbit at $\mu = \mu_c$ ($\mu_c \cong 0.90032$) with $\mu < \mu_c$, $x \sim \mu t$, $y \to 0$ as $t \to \infty$ from all initial conditions. We now consider the solution near the bifurcation points at $\mu = \mu_1$ and $\mu = \mu_2$.

3. Behaviour near the bifurcation points

To study the behaviour of the solutions of equation (5) near the points of Hopf bifurcation $\mu = \mu_1$ and $\mu = \mu_2$ we use the method of multiple scales, Jordan and Smith [13]. The details are similar to those described in Merkin et al. [14] and need not be repeated in full here. We find it more convenient to use $\xi = x + y$ and y as dependent variables, and put

$$\mu = \mu_i \pm \epsilon^2 \quad (i = 1, 2) \tag{9}$$

(where the + sign is taken with μ_1 and the − sign with μ_2). An expansion of ξ and y in the form

$$\xi = \xi_s + \epsilon\xi_1 + \epsilon^2\xi_2 + \epsilon^3\xi_3 + \cdots, \quad y = y_s + \epsilon y_1 + \epsilon^2 y_2 + \epsilon^3 y_3 + \cdots \tag{10}$$

where $\xi_s = x_s + y_s$, leads to secular terms at $O(\epsilon^3)$ which we remove by introducing the the slow time variable $\tau = \epsilon^2 t$. Then

$$y_1 = A(\tau)\cos(\omega_i t + \phi(\tau)), \quad \xi_1 = -\frac{A(\tau)}{\omega_i}\sin(\omega_i t + \phi(\tau)) \tag{11}$$

where

$$\omega_1^2 = \frac{1}{2}\left(1 - \sqrt{1 - \frac{8}{\rho}}\right), \quad \omega_2^2 = \frac{1}{2}\left(1 + \sqrt{1 - \frac{8}{\rho}}\right). \tag{12}$$

To remove the secular terms at $O(\epsilon^3)$ the amplitude $A(\tau)$ must satisfy

$$\frac{dA}{d\tau} = \frac{\mu_1}{\omega_1^2}\left(1 - \frac{8}{\rho}\right)^{1/2} A\left(1 - \frac{A^2}{D_1^2}\right) \tag{13}$$

for μ close to μ_1 and

$$\frac{dA}{d\tau} = \frac{\mu_2}{\omega_2^2}\left(1 - \frac{8}{\rho}\right)^{1/2} A\left(1 - \frac{A^2}{D_2^2}\right) \tag{14}$$

for μ close to μ_2. In these equations

$$\frac{1}{D_1^2} = \frac{3\omega_1^2}{8\mu_1\left(1 - \frac{8}{\rho}\right)^{1/2}} + \frac{\left\{11 + 5\left(1 - \frac{8}{\rho}\right)^{1/2}\right\}\mu_1}{4\omega_1^2\left\{7 + \left(1 - \frac{8}{\rho}\right)^{1/2}\right\}} \tag{15}$$

and

$$\frac{1}{D_2^2} = \frac{3\omega_2^2}{8\mu_2\left(1 - \frac{8}{\rho}\right)^{1/2}} - \frac{\left\{11 - 5\left(1 - \frac{8}{\rho}\right)^{1/2}\right\}\mu_2}{4\omega_2^2\left\{7 - \left(1 - \frac{8}{\rho}\right)^{1/2}\right\}}. \tag{16}$$

Clearly $D_1^2 > 0$ for all $\rho > 8$ and also it is relatively straightforward to show, using (7) and (12), that $D_2^2 > 0$ for all $\rho > 8$.

From equations (13) and (14) it follows that $A \to D_i$ as $\tau \to \infty$ from any (positive) initial conditions, so that defining the amplitudes A_x and A_y of the oscillations in x and y respectively by $A_x = x_{\max} - x_{\min}$ and $A_y = y_{\max} - y_{\min}$, we have

$$A_x = \frac{2D_i}{\omega_i}\left(1 + \omega_i^2\right)^{1/2}|\mu - \mu_i|^{1/2} + \cdots, \quad A_y = 2D_i|\mu - \mu_i|^{1/2} + \cdots \quad (i = 1, 2) \tag{17}$$

for $|\mu - \mu_i| \ll 1$. For $\rho \gg 1$ we have from (12) that

$$\omega_i \sim \sqrt{2}\,\rho^{-1/2} + \cdots, \quad \omega_2 = 1 - \rho^{-1} + \cdots. \tag{18}$$

On using these in the expressions for D_1 and D_2 we have, for $\rho \gg 1$, that near $\mu = \mu_1$

$$A_x \sim 2\sqrt{2}\,\rho^{1/4}(\mu - \mu_1)^{1/2} + \cdots, \quad A_y \sim 4\rho^{-1/4}(\mu - \mu_1)^{1/2} + \cdots, \tag{19}$$

and near $\mu = \mu_2$

$$A_x \sim 8(\mu_2 - \mu)^{1/2} + \cdots, \quad A_y \sim 4\sqrt{2}\,(\mu_2 - \mu)^{1/2} + \cdots. \tag{20}$$

So from (18) and (20) we can see that both the amplitude and period of the oscillations close to $\mu = \mu_2$ remains bounded and in fact approaches the expressions given by Merkin et al. [7] (where the uncatalysed step was not included) as $\rho \to \infty$. From (18) and (19) we see that near $\mu = \mu_1$ the period of the oscillations and A_x grow large for large ρ while A_y becomes small.

Also, we note that both D_1^2 and D_2^2 remain positive for all $\rho > 8$ and so the bifurcations at both $\mu = \mu_1$ and $\mu = \mu_2$ do not change in character, producing a stable limit cycle in $\mu > \mu_1$ and $\mu < \mu_2$ respectively. This last point has been checked numerically using the bifurcation program given by Hassard et al. [15]. The next step is to show that (x_s, y_s) is surrounded by at least one stable limit cycle for each μ in $\mu_1 < \mu < \mu_2$.

4. The phase portrait

Here we extend the results of the previous section by showing that for each μ in $\mu_1 < \mu < \mu_2$ (with $\rho > 8$) there is at least one limit cycle surrounding (x_s, y_s) in the quadrant $x, y > 0$.

First we note that, since $\mathrm{d}x/\mathrm{d}t = \mu > 0$ on $x = 0$ and $\mathrm{d}y/\mathrm{d}t = x/\rho \geqslant 0$ on $y = 0$ (with $x \geqslant 0$), all paths must enter the quadrant $x, y \geqslant 0$ with increasing t. So all trajectories with initial conditions $x_0, y_0 \geqslant 0$ *remain* in $x, y \geqslant 0$ for all t. We now show that such trajectories must also remain bounded in $t > 0$ (i.e. they cannot be attracted to infinity in this quadrant). This is done by examining the phase portrait of equations (5) as $x, y \to \infty$.

To discuss the behaviour at infinity we use the Poincaré projection, Jordan and Smith [13], introducing new variables

$$\mu = \frac{y}{x}, \quad v = -\frac{1}{x}. \tag{21}$$

Transformation (21) maps the quadrant $x, y > 0$ bijectively onto the quadrant $u > 0$, $v < 0$ in the (u, v) plane and is constructed so that the lines $y/x =$ constant as $x \to \infty$ are mapped into the lines $u =$ constant as $u \to 0^-$. So the behaviour near the 'arc at infinity' $x^2 + y^2 \to \infty$ is mapped into the neighbourhood of the line $v = 0^-$ in the (u, v) plane. We can discuss the behaviour of paths at infinity in the (x, y) plane by examining the corresponding paths in the finite (u, v) plane (the point at infinity on the y-axis is also mapped to infinity in the (u, v) plane and this point has to be considered separately).

In terms of u and v, equations (5) can be combined to give the first-order equation

$$\frac{\mathrm{d}v}{\mathrm{d}u} = \frac{v(\mu v^3 + u^2 + v^2/\rho)}{u(u - v^2 + \mu v^3 + u^2) + (1 + u)v^2/\rho}. \tag{22}$$

Equilibrium points in the first quadrant of the (x, y) plane as $x^2 + y^2 \to \infty$ must have $v = 0$, and from (22)

$$u^2(1 + u) = 0, \quad u \geqslant 0. \tag{23}$$

The only solution of (23) is $u = 0$ which corresponds to an equilibrium point in the (x, y) plane at the positive 'end' of the x-axis (so the inclusion of the extra step (4) does not introduce any

extra equilibrium points at infinity). Also, $v=0$, $u>0$ is a phase path of (22) which corresponds through (21) to a bounding path at infinity in x, $y \geqslant 0$ joining the equilibrium point at the positive end of the x-axis to that at the positive end of the y-axis.

Next consider the nature of the phase paths determined by (22) in the neighbourhood of the equilibrium point $u=v=0$. The horizontal isocline is given by the curve

$$u=\left(-\mu v^3-\frac{v^2}{\rho}\right)^{1/2}, \quad v \leqslant 0, \quad u \geqslant 0, \tag{24}$$

which is defined only for $v \leqslant -1/(\mu\rho)$ and is a monotone decreasing function of v. So in some sufficiently close neighbourhood of $u=v=0$, $\mathrm{d}v/\mathrm{d}u \neq 0$. The vertical isocline is given implicitly by

$$u\left\{u-\left(1-\frac{1}{\rho}\right)v^2+\mu v^3+u^2\right\}+\frac{v^2}{\rho}=0. \tag{25}$$

It is clear from (25) that $u=u(v)$ has two branches in $u \geqslant 0$, $v \leqslant 0$. To obtain a uniform approximation to the solution of (25) for $\rho \gg 1$ we begin on the lower branch where u is of $O(\rho^{-1})$ and v is of O(1), and look for a solution in the form

$$u(v;\rho)=\rho^{-1}u_1(v)+\rho^{-2}u_2(v)+\cdots. \tag{26}$$

Substituting (26) into (25), expanding and solving upto $O(\rho^{-2})$ gives

$$u(v;\rho)=\frac{\rho^{-1}}{1-\mu v}+\frac{1+v^2(1-\mu v)}{v^2(1-\mu v)^3}\rho^{-2}+O(\rho^{-3}). \tag{27}$$

Expansion (27) becomes non-uniform as $v \to 0^-$, in particular when v is of $O(\rho^{-1/2})$ (which gives u of $O(\rho^{-1})$). To continue the solution we introduce the scaled variable V given by $v=\rho^{-1/2}V$ where V is now of O(1). In terms of u and V, equation (25) becomes

$$u\left\{u-\left(1-\frac{1}{\rho}\right)\frac{V^2}{\rho}+\frac{\mu}{\rho^{3/2}}V^3+u^2\right\}+\frac{V^2}{\rho^2}=0. \tag{28}$$

We look for a solution of (28) in the form

$$u(V;\rho)=\rho^{-1}u_1(V)+\cdots. \tag{29}$$

At leading order we obtain

$$u_1=\tfrac{1}{2}\left(V^2 \pm V\sqrt{V^2-4}\right). \tag{30}$$

For $V<0$, (30) is defined for $-\infty < V \leqslant -2$, and $u_1 \sim 2\{1 \mp \sqrt{-(V+2)}\}$ as $V \to -2$ from below. So we have

$$u(V;\rho)=\tfrac{1}{2}\left\{V^2 \pm V\sqrt{V^2-4}\right\}\rho^{-1}+O(\rho^{-3/2}). \tag{31}$$

With the $-$ sign taken in (30), the solution as $V \to -\infty$ matches with (27) as $v \to 0^-$ giving the continuation of the lower branch, then (31) turns this lower branch (27) round at $V=-2$.

Expansion (31) becomes non-uniform on the upper branch (with the $+$ sign now taken) when V is of $O(\rho^{1/2})$ i.e. when v is of O(1). So to continue the upper branch we look for a solution of (25) in the form

$$u(v;\rho)=u_0(v)+u_1(v)\rho^{-1}+\cdots, \tag{32}$$

giving at leading order

$$u_0 = \tfrac{1}{2}\left\{-1 + \sqrt{1 + 4(v^2 - \mu v^3)}\right\}, \quad v < 0, \tag{33}$$

where the positive sign is taken for the square root to make $u_0 > 0$ when $v < 0$. Hence we have

$$u(v;\, \rho) = \tfrac{1}{2}\left\{-1 + \sqrt{1 + 4(v^2 - \mu v^3)}\right\} + O(\rho^{-1}). \tag{34}$$

Expansion (34) matches with the upper branch of (30) as $v \to 0^-$, $V \to -\infty$ respectively.

The three expansions (27), (31) and (34) provide a uniform approximation to the vertical isocline in $v \leqslant 0$, $u \geqslant 0$. The isoclines can now be sketched, as shown in Fig. 2(a). From this figure we can infer immediately that, sufficiently close to $u = v = 0$, $dv/du < 0$, with, from (22), that $dv/dt < 0$, $du/dt > 0$. Also, we have that on $u = 0$, $dv/du \sim v$, $v \to 0^-$. We are now in a

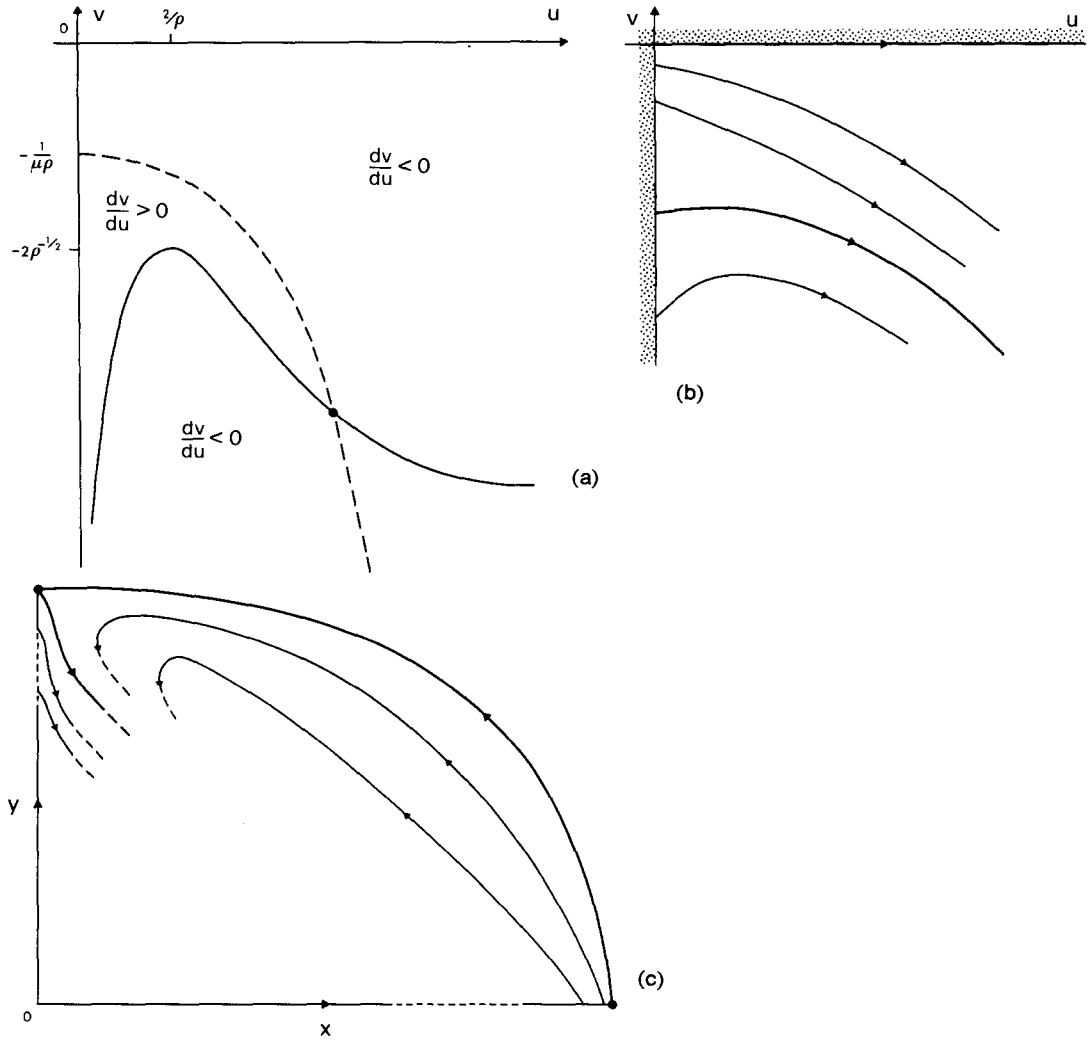

Fig. 2. The phase plane at infinity: (a) the isoclines in the (u, v) plane; the vertical isocline is shown by a continuous line, the horizontal isocline by a broken line, (b) the trajectories near $u = 0$, $v = 0$ in the (u, v) plane, (c) the phase portrait in the (x, y) plane.

position to give a qualitative sketch of the phase paths in the (u, v) plane close to $u = v = 0$. These are shown in Fig. 2(b). The important point to note is that all paths enter the region $u > 0$, $v \leqslant 0$ with increasing t and *no* paths starting in $u \geqslant 0$, $v \leqslant 0$ (except $u \equiv v \equiv 0$) can approach $u = v = 0$, i.e. the equilibrium point $u = v = 0$ is unstable.

To complete the phase portrait at infinity it remains to examine the behaviour in the neighbourhood of the y-axis as $y \to \infty$. This is done through a transformation similar to (21). As expected, since the term x/ρ will be negligible for $y \gg 1$, $x \ll 1$, the details of the phase portrait at the positive 'end' of the y-axis are qualitatively the same as those given by Merkin et al. [7] when the uncatalysed step is absent. Thus we find that there is an equilibrium point at the 'end' of the y-axis which is a saddle-point. The stable separatrix of which forms the extension of the bounding path at infinity, while the unstable separatrix enters $x, y > 0$. The complete phase portrait at infinity can now be sketched and is shown in the (x, y) plane in Fig. 2c.

The examination of the phase portrait at infinity has shown the existence of a bounding path connecting two *unstable* equilibrium points. So no paths starting in $x, y \geqslant 0$ can be attracted to infinity and we can conclude that all such paths must remain *bounded* for $t > 0$.

With this result, a straightforward application of the Poincaré-Bendixson theorem (Jordan and Smith [13]) shows that there will be at least one stable limit cycle in $x, y > 0$ (which must surround (x_s, y_s) whenever (x_s, y_s) is unstable. In fact there must be an odd number of limit cycles, with the innermost and outermost ones both being stable. Therefore, at each μ in $\mu_1 < \mu < \mu_2$, equations (5) have at least one stable limit cycle. Numerical integrations of equations (5), as described in the next section, were performed for a wide range of initial values (and values of μ and ρ) and these indicate that there is just one such limit cycle in $\mu_1 < \mu < \mu_2$ and no limit cycles outside this range. (We can show by direct integration that there are no oscillatory solutions at $\mu = 0$).

Finally it is of interest to note that bounds may be put on $x_{\max}$ for these limit cycles. A sketch of the horizontal and vertical isoclines of equations (5) is given in Fig. 3 from which it is clear that

$$x_s < x_{\max} < \mu\rho. \tag{35}$$

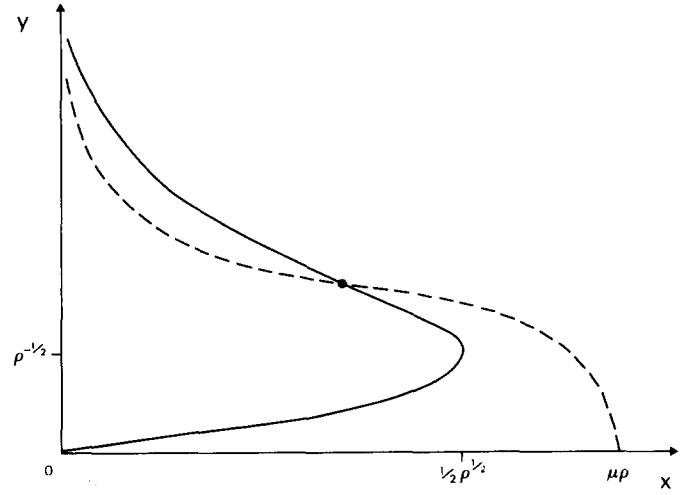

Fig. 3. A sketch of the isoclines of equations (5); the vertical isocline is shown by a continuous line, the horizontal isocline by a broken line.

5. Numerical results

Equations (5) were solved numerically using a Runge-Kutta method for several values of ρ and a range of μ in the interval $\mu_1 < \mu < \mu_2$. The numerical solution started close to (x_s, y_s), integrating forwards in t with a step length Δt typically $\Delta t = 0.05$ until the solution settled onto a limit cycle (which was deemed to have been achieved when the solution had repeated itself over more than 30 cycles). A graph of A_x (defined by $A_x = x_{\max} - x_{\min}$) against μ for $\rho = 20$ is shown in Fig. 4. The graph of A_y (defined by $A_x = y_{\max} - y_{\min}$) is similar to this and is not shown. There is a smooth curve rising from zero at $\mu = \mu_1$ to a maximum value of approximately 2.96 before decreasing to zero against at $\mu = \mu_2$. This is typical of the behaviour of limit-cycle amplitudes for moderate values of ρ. For increased ρ the picture changes, a graph of A_x against μ for $\rho = 200$ is shown in Figure 5(a). Here we can see that close to μ_2 the behaviour is similar to that given by Merkin et al. [7]. However, around $\mu = \mu_c$ ($\cong 0.90032$), where without the uncatalysed step the amplitude becomes unbounded, A_x grows rapidly, reaching a maximum of approximately 10.22. As μ is decreased further, this value slowly decreases until close to μ_1 it drops rapidly to zero. To the accuracy of the plotting in Fig. 5(a) it appears to decrease discontinuously to zero, and to see this behaviour more clearly the values of A_x close to $\mu = \mu_1$ were also calculated, starting at $\mu_1 + \Delta\mu$, where $\Delta\mu = (\mu_2 - \mu_1)/12\,500 = 7.368 \times 10^{-5}$ and increasing μ in steps of $\Delta\mu$. These are shown in Fig. 5(b) (The detail around where there is a rapid increase in A_x was examined in finer detail using an even smaller value of $\Delta\mu$). Here we can see that very close to μ_1 the solution has the form as given from the Hopf bifurcation theorem by (19), but this is followed by a very rapid rise to the values as shown in Fig. 5(a). A graph of A_y against μ for $\rho = 200$ is shown in Fig. 5(c). Here again we can see the rapid rise in A_y around $\mu = \mu_c$, reaching a maximum value of approximately 7.09, but here A_y decreases smoothly to zero at $\mu = \mu_1$.

The period t_p of the limit cycles for $\mu_1 < \mu < \mu_2$ and $\rho = 200$ is plotted in Fig. 5(d) the values of t_p close to μ_2 are consistent with (18), there is a fairly rapid rise in t_p around $\mu = \mu_c$ followed by an increase in t_p over the rest of the range. The values close to $\mu = \mu_1$ appear to be at odds with (18) (this gives a value $t_p = 62.8$ at μ_1). Values very close to μ_1 are shown in the inset of this figure where we can again see (as in Figs. 5(a) and 5(b)) the rapid change from the value as given by the Hopf bifurcation. The very rapid rise in A_x around to $\mu = \mu_c$ can be seen even more clearly in Fig. 6, where A_x is plotted against μ for $\rho = 2000$.

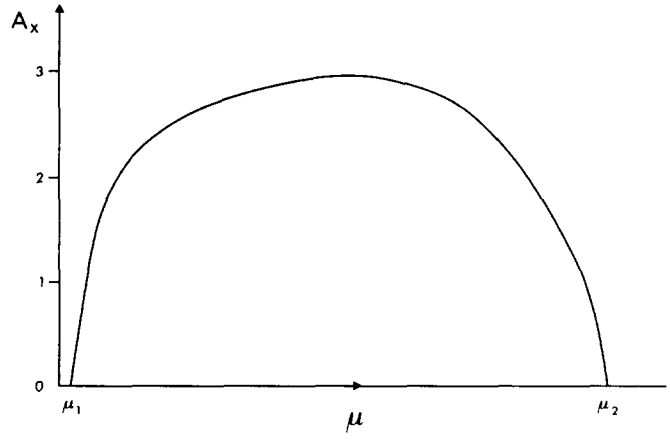

Fig. 4. A graph of the amplitude A_x against μ for $\rho = 20$, $\mu_1 = 0.2504$, $\mu_2 = 0.9150$.

It is interesting to note that, for a given value of μ, the mean value of y over a period is the same for all ρ. On adding equations (5) we get $d\xi/dt = \mu - y$, where $\xi = x + y$, then integrating this over a period t_p gives

$$\frac{1}{t_p}\int_0^{t_p} y \, dt = \mu = y_s.$$

Further quantitative information about the solution near $\rho = 8$ than was given by Golubitsky and Langford [12] can be obtained by expanding about $\rho = 8$ and using the method of multiple scales. To do this we first put

$$\xi = x + y = \mu + \frac{\mu}{\mu^2 + 1/\rho} + X, \quad y = \mu + Y, \tag{36}$$

then with $\rho = 8 + \delta$, $\delta \ll 1$, we expand μ, X, and Y in the form

$$\begin{aligned} \mu &= \mu_0 + \delta^{1/2}\nu_1 + \delta\nu_2 + \cdots, \\ X &= \delta^{1/2}X_1 + \delta X_2 + \delta^{3/2}X_3 + \cdots, \\ Y &= \delta^{1/2}Y_1 + \delta Y_2 + \delta^{3/2}Y_3 + \cdots, \end{aligned} \tag{37}$$

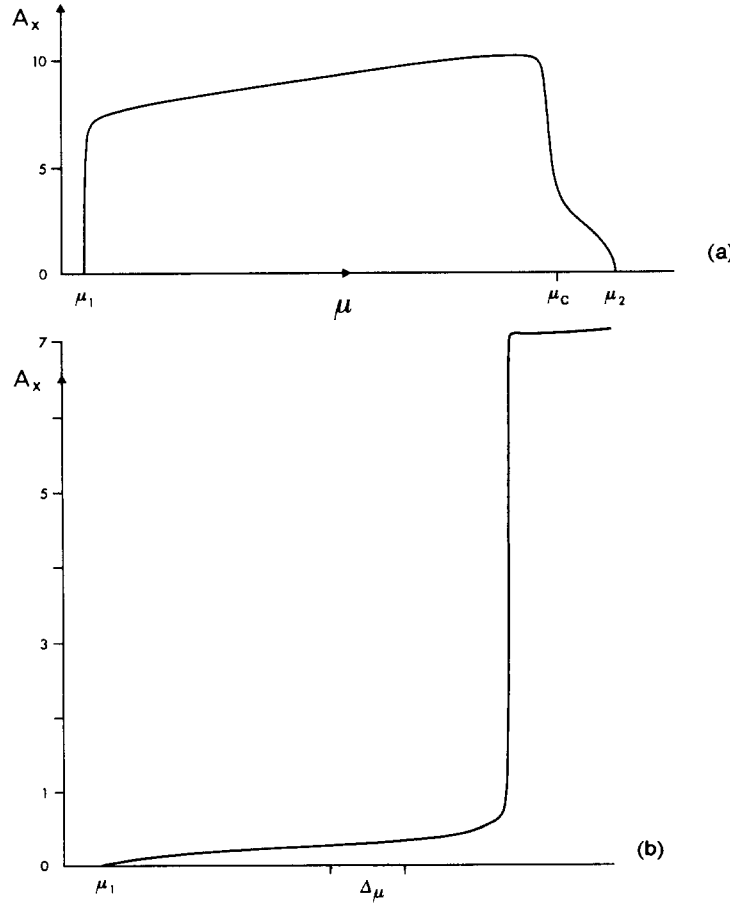

Fig. 5. The behaviour for $\rho = 200$, $\mu_1 = 0.0714$, $\mu_2 = 0.9924$: (a) the amplitude A_x plotted against μ, (b) the amplitude A_x close to μ_1, $\Delta\mu = 7.368 \times 10^{-5}$, (c) the amplitude A_y plotted against μ, (d) the period t_p plotted against μ.

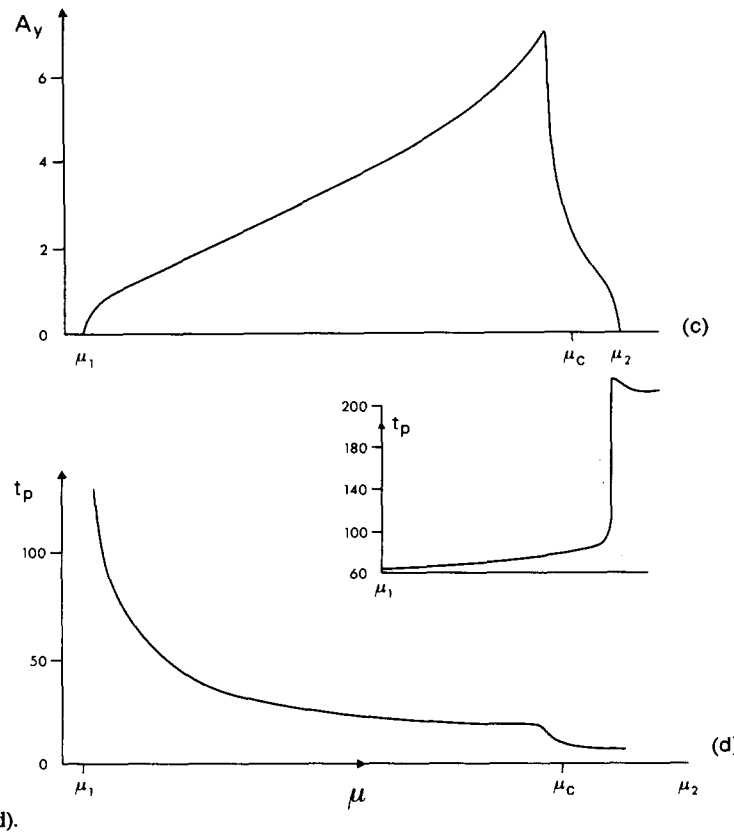

Fig. 5 (continued).

where $\mu_0 = \sqrt{3/8}$ is the value of μ_1 and μ_2 at $\rho = 8$. The expansion in powers of $\delta^{1/2}$ is suggested by the forms of μ_1 and μ_2 near $\rho = 8$. When (36) and (37) are substituted into equations (5) and the resulting hierarchy of equations solved we find that secular terms arise at $O(\delta^{3/2})$. These are removed by introducing the slow time $\tau = \delta t$, and so we have at $O(\delta^{1/2})$:

$$X_1 = -\sqrt{2}A(\tau)\sin\left\{\frac{t}{\sqrt{2}} + \phi(\tau)\right\}, \quad Y_1 = A(\tau)\cos\left\{\frac{t}{\sqrt{2}} + \phi(\tau)\right\}. \tag{38}$$

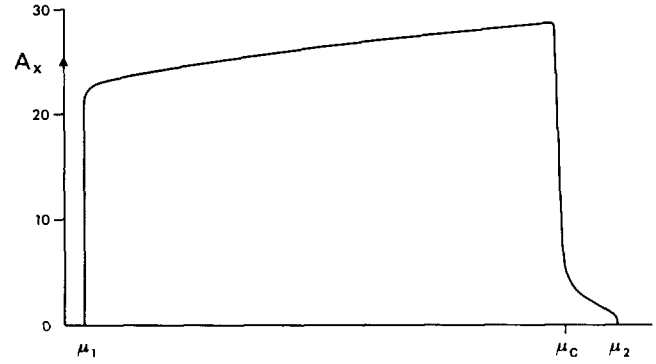

Fig. 6. A graph of the amplitude A_x plotted against μ for $\rho = 2000$, $\mu_1 = 0.0224$, $\mu_2 = 0.9992$.

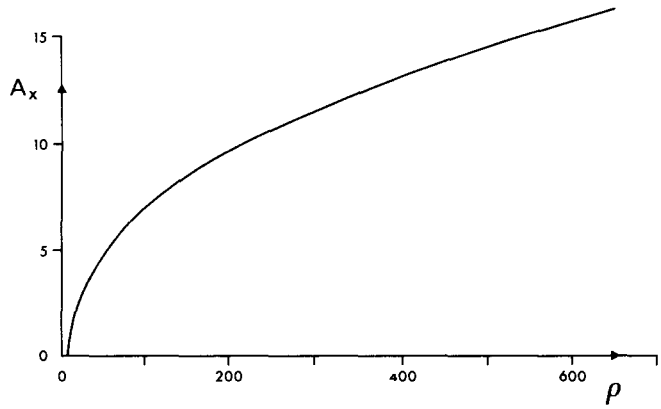

Fig. 7. A graph of the amplitude A_x against ρ for $\mu = \mu_0 = \sqrt{3/8}$.

To remove the secular terms at $O(\delta^{3/2})$, we find after some algebra that the amplitude $A(\tau)$ must satisfy the equation

$$\frac{dA}{d\tau} = \frac{1-48\nu_1^2}{32}A\left(1 - \frac{12}{1-48\nu_1^2}A^2\right). \tag{39}$$

For $\nu_1^2 > 1/48$, equation (39) has only the one stationary state $A = 0$ and it is easy to show that this is stable. For $\nu_1^2 < 1/48$, equation (39) has two possible stationary states, namely $A = 0$ and $A = A_e = \{(1-48\nu_1^2)/12\}^{1/2}$. Again it is straightforward to show $A = 0$ is unstable and that $A = A_e$ is stable, so that a stable limit cycle exists only for $-1/\sqrt{48} < \nu_1 < 1/\sqrt{48}$.

Finally we have from the above solution that A_x and A_y are both of $O((\rho-8)^{1/2})$ close to $\rho = 8$, and in particular with $\mu = \mu_0 = \sqrt{3/8}$ we find that

$$A_x = (\rho-8)^{1/2} + \cdots, \quad A_y = \frac{1}{\sqrt{3}}(\rho-8)^{1/2} + \cdots \tag{40}$$

for $(\rho - 8) \ll 1$. Values of A_x for $\rho > 8$ have been calculated numerically keeping μ fixed at μ_0. A graph of A_x against ρ is shown in Fig. 7, where the singular behaviour, given by (40), near $\rho = 8$ can clearly be seen.

6. Discussion

The numerical results show that for $\rho \gg 1$ and μ close to μ_1 and μ_2 the amplitudes of the limit cycles are as given by Hopf bifurcation theorem, (19) and (20). Near $\mu = \mu_2$, where a bounded solution exists for $\mu_c < \mu$ even without the addition of the uncatalysed reaction, the limit cycle behaviour follows closely that given by Merkin et al. [7], so that the effect of the extra step is unimportant. However, for $\mu < \mu_c$, the addition of the uncatalysed reaction (even though this is very slow compared to the autocatalytic step) is vital in keeping the solution bounded and preserving the validity of the pooled chemical approximation.

Near $\mu = \mu_1$, the amplitudes A_x and A_y are, for $\rho \gg 1$, as given by (19), though this behaviour is confined to a narrow range very close to μ_1, and these expressions are of little use in estimating the amplitudes for μ away from μ_1. To see why this is the case we note that (35) suggests that A_x is at least of $O(\rho^{1/2})$ for $\rho \gg 1$, whereas the solution close to μ_1 gives A_x as $O(\rho^{1/4})$, from (19), so there must be a rapid change from this lower value to the higher one

close to μ_1. For μ such that $\mu < \mu_1$ and $\mu > \mu_2$ the stationary state (x_s, y_s) as given by (6) is stable and the solution approaches this state from all (positive) initial conditions as $t \to \infty$.

In terms of the chemical reaction scheme (1–4), we can see that without step (4) there is a parameter range where it is possible for B to decay more quickly to C via step (3) than can be produced from A via step (2). With the supply of B completely exhausted, all that is left is step (1) which just produces A from P. The inclusion of the uncatalysed reaction (4) stops this happening, B is always being produced from A via this step, and even though the concentration of B can get very small it can never be totally used up. This then enables the much faster autocatalytic step (2) to keep producing B from A, slowly at first when the concentration of B is low, but as the concentration of B builds up this rate of production increases rapidly until virtually all A has been used up. Reaction (2) then slows down again, allowing A to build up via (1) with B decreasing via step (3) and the whole process can then be repeated.

References

1. P. Gray and S.K. Scott: Autocatalytic reactions in the isothermal continuous stirred tank reactor: isolas and other forms of multistability. *Chem. Engng. Sci.* 38 (1983) 29–43.
2. P. Gray and S.K. Scott: Autocatalytic reactions in the continuous stirred tank reactor: oscillations and instabilities in the system $A + 2B \to 3B$; $B \to C$. *Chem. Engng. Sci.* 39 (1984) 1087–1097.
3. P. Gray and S.K. Scott: Sustained ocsillations and other exotic patterns of behaviour in isothermal reactions. *J. Phys. Chem.* 89 (1985) 22–32.
4. S.K. Scott: Reversible autocatalytic reactions in an isothermal CSTR. *Chem. Engng. Sci.* 38 (1983) 1701–1708.
5. A. D'Anna, P.G. Lignola and S.K. Scott: The application of singularity theory to isothermal autocatalytic open systems: the elementary scheme $A + mB \to (m+1)B$. *Proc. Roy. Soc.* A403 (1986) 341–363.
6. J.H. Merkin, D.J. Needham and S.K. Scott: Oscillatory chemical reactions in closed vessels. *Proc. Roy. Soc.* A406 (1986) 299–323.
7. J.H. Merkin, D.J. Needham and S.K. Scott: On the creation, growth and extinction of oscillatory solutions for a simple pooled chemical reaction scheme. To be published in *SIAM J. on Applied Mathematics.*
8. B.F. Gray, S.K. Scott and P. Gray: Multiplicity for isothermal autocatalytic reactions in open systems: the influence of reversibility and detailed balance. *J. Chem. Soc. Faraday Trans.* 1 80 (1984) 3409–3417.
9. B.F. Gray and S.K. Scott: Multistability and sustained oscillations in isothermal open system. *J. Chem. Soc. Faraday Trans.* 1 81 (1985) 1563–1567.
10. J. Tyson and S. Kauffman: Control of mitosis by a continuous biochemical oscillation: synchronisation; spatially inhomogeneous oscillations. *J. Math. Biology* 1 (1975) 289–310.
11. M.Ashkenazi and H.G. Othmer: Spatial patterns in coupled biochemical oscillators. *J. Math. Biology* 5 (1978) 305–350.
12. M. Golubitsky and W.F. Langford: Classification of degenerate Hopf bifurcations. *J. Diff. Equations* 41 (1981) 375–415.
13. D.W. Jordan and P. Smith: *Nonlinear ordinary differential equations.* Oxford University Press (1983).
14. J.H. Merkin, D.J. Needham and S.K. Scott: A simple model for sustained oscillations in isothermal branched-chain or autocatalytic reactions in a well stirred open system, II: limit cycles and nonstationary states. *Proc. Roy. Soc.* A398 (1985) 101–116.
15. B.D. Hassard, N.D. Kazarinoff and Y.-H. Wan: *Theory and applications of Hopf bifurcation*, (London Mathematical Society Lecture Notes Series No. 41, edited by I.M. James), Cambridge University Press (1981).